Coastal Engineering 121 (2017) 255–264

Contents lists available at ScienceDirect

Coastal Engineering

journal homepage: www.elsevier.com/locate/coastaleng

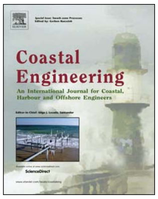

Momentum transfer under laboratory wind waves

M. Olfateh, P. Ware, D.P. Callaghan, P. Nielsen, T.E. Baldock*

School of Civil Engineering, The University of Queensland, Brisbane, Australia

ARTICLE INFO

MSC:
00-01
99-00

Keywords:
Wind-waves
Momentum
Reynolds
Organised
Motion

ABSTRACT

In this study, we explain contradictory previous observations of the contribution of coherent wave organised motion to the downward transfer of momentum through wave Reynolds stresses ($\rho\overline{\tilde{u}\tilde{w}}$) below wind waves. The generation of non-zero $\overline{\tilde{u}\tilde{w}}$ is potentially significant because 1) the turbulent mixing is not then the only momentum transport mechanism under wind waves as was previously assumed, 2) this provides a wave-current energy exchange pathway that could explain inconsistencies in measured air- and water-side wind-wave energy transfer and 3) it can be a critical term in the wave-current coupling formulation under wind waves. However, such a mechanism for momentum transfer has generally been ignored, since contradictory observations were reported. Here, two new sets of wind-wave laboratory experiments are reported. For the first set, contradictory $\overline{\tilde{u}\tilde{w}}$ were observed, as in previous literature. Investigating the sources of such inconsistency, we examined spatial inhomogeneity due to wave reflection through a second set of experiments, by varying instrument location and additionally considering random waves. The results resolve the inconsistencies observed in the first set of experiments and previous measurements. In addition, we emphasise the contribution of secondary circulation cells in momentum transfer under wind waves.

1. Introduction

Viscous and Reynolds stresses transfer horizontal momentum vertically throughout the air- and water-side of an atmosphere-ocean boundary layer. Below gravity waves, the organised wave motion velocities $\tilde{\mathbf{u}} = (\tilde{u}, \tilde{v}, \tilde{w})$ add to the conventional Reynolds decomposition and introduce $\rho\overline{\tilde{u}\tilde{w}}$ as the wave Reynolds stress component in the $x - z$ plane of a (x, y, z) Cartesian coordinate system [29]. Here, x is along the long-crested wave propagation direction, y is along the wave crest, z is vertically upward with origin at the mean water surface and $\overline{f}$, $\tilde{f}$ and f' are the mean, periodic and turbulent components of time series f. Therefore, the total shear stress is $\tau_{xz} = \mu\frac{du}{dz} - \rho\overline{\tilde{u}\tilde{w}} - \rho\overline{u'w'}$ in a 2D scenario (i.e. $v = 0$) assuming $\overline{\tilde{u}w'}$, $\overline{u'\tilde{w}}$, $\overline{\mathbf{u}}'$ and $\overline{\tilde{\mathbf{u}}}$ zero where μ and ρ are the fluid dynamic viscosity and density, respectively.

Although linear and non-linear solutions for uniform gravity waves over a horizontal bottom give $\tilde{u}$ and $\tilde{w}$ in quadrature [7], and thus $\overline{\tilde{u}\tilde{w}} = 0$, several specific solutions show that $\overline{\tilde{u}\tilde{w}} \neq 0$ under certain conditions [26,20,28,8,30]. For instance, Nielsen et al. [26] showed that for spatially growing shallow water waves orbital velocities go out of quadrature and the organised wave motion transfers momentum downwards in the water column. The shear stress $\tau_{xz} = -\rho\overline{\tilde{u}\tilde{w}}$ is then in equilibrium with $\frac{\partial}{\partial x}\rho\overline{\tilde{u}^2}$, since the mean water surface elevation is assumed flat. In an alternative approach, Mellor [20] introduced the shear stress from a subsurface projection of the wave-coherent pressure correlated to the material slope. Mellor [20] assumed that the material surface was the same as in free waves by using the Rayleigh drag as a momentum sink (i.e. negligible spatial and temporal wave growth). Using the conservation of momentum, Mellor showed that the shear stress is equivalent to $-\rho\overline{\tilde{u}\tilde{w}}$.

Analogous to growing wind-waves, analytical studies found $-\rho\overline{\tilde{u}\tilde{w}} \neq 0$ for shoaling waves [30] and decaying waves [28,8]. For decay due to the viscous stresses in the bottom boundary layer, the rotational and irrotational wave motion are correlated, transferring momentum upward, as in Phillips [28, pp. 33-41]. For a surface source of dissipation, such as surface rollers of breaking waves, Deigaard and Fredsøe [8] derived a linear depth distribution for $\overline{\tilde{u}\tilde{w}}$ for shallow water. Rivero and Arcilla [30] investigatd the depth distribution of $\overline{\tilde{u}\tilde{w}}$ for shoaling waves on a sloping bed with and without a bed boundary layer. The linear depth distribution of $\overline{\tilde{u}\tilde{w}}(z)$ in shallow water found by Deigaard and Fredsøe [8] and Rivero and Arcilla [30] are consistent.

Several experimental studies have observed $\overline{\tilde{u}\tilde{w}} \neq 0$ under wind waves. These studies (discussed in detail in Section 2) are not in agreement, by which we mean that positive, negative and extraordinarily large (compared to the wind momentum input) wave Reynolds stresses have been measured. It seems that these inconsistencies have negated the potential impacts of such findings, which if proven to be right, are very significant. This is because the turbulent Reynolds stress is not then the only mechanism for transferring surface wind momen-

---

* Corresponding author.
E-mail address: t.baldock@uq.edu.au (T.E. Baldock).

http://dx.doi.org/10.1016/j.coastaleng.2016.09.001
Received 20 April 2016; Received in revised form 1 September 2016; Accepted 3 September 2016

Table 1
Experimental measurements of $\dot{E}_w/\dot{E}_t$ indicating a significant part of the total momentum input is transferred into waves.

Study	$\dot{E}_w/\dot{E}_t$	Remarks
Snyder et al. [34]	0.3-0.9	Air-side field measurements
Hsu et al. [11]	0.6	Air-side wave flume measurements
Mitsuyasu [22]	*ca.* 0.55	Analytically estimation from measurements of Mitsuyasu and Honda [23]
Mastenbroek et al. [19]	0.6-0.8	Laboratory experiments
Liberzon and Shemer [15]	0.1-0.6	Air-side and wave growth measurements in wave tank
Grare et al. [10]	0.5-0.9	Wave growth data from wave tank

tum into the water column [14,21]. In addition, $\overline{\tilde{u}\tilde{w}} \neq 0$ provides a mechanism for a wave-current energy exchange, through the term $\overline{\tilde{u}\tilde{w}}\frac{\partial u}{\partial z}$, under wind waves [29]. This is important for modelling both wind wave generation and wave-current coupling under wind waves. Despite the fact that several wind-wave experiments have measured significant portions of the total wind energy, $\dot{E}_t$, being initially transferred into waves, $\dot{E}_w$, (Table 1), concurrent wave growth measurements underestimate this air-side measured wind energy input by a factor of 2 to 3 [10,15]. Noting the extraordinarily large measurement of $\overline{\tilde{u}\tilde{w}}$ by Cheung and Street [6], $\overline{\tilde{u}\tilde{w}}\frac{\partial u}{\partial z}$ was suggested by Grare et al. [10] as a possible sink for wind energy transferred to the waves.

Considering the potential significance of the occurrence of $\overline{\tilde{u}\tilde{w}} \neq 0$ under wind waves, which can be supported theoretically, the contradictory experimental literature demands an explanation. The present paper considers this issue and determines if $\overline{\tilde{u}\tilde{w}}$ are actually non-zero under wind waves. This paper is organised as follows. The literature, i.e. previous experimental observations of $\overline{\tilde{u}\tilde{w}}$, are reviewed in Section 2. We present results from two new sets of wind-wave laboratory experiments in Section 3. In the first set of experiments, the previous inconsistencies were again observed, discussed in Section 4. In Section 5 we analyse and discuss the impact of wave reflection in wind wave flumes. The second set of experiments was performed to account for the effects of wave reflection. These results are presented in Section 6 and clarify the previous observations. Final conclusions are given in Section 7.

2. Previous experimental results

As noted above, previous experiments reported non-zero, and in some cases extraordinarily large (compared to the expected wind momentum flux), wave Reynolds stresses under wind waves by measuring out of quadrature $\tilde{u}$ and $\tilde{w}$. This procedure demands decomposition of the measured velocity time series. In this process, time averaging over a long-enough duration separates out $\bar{\mathbf{u}}$. Phase averaging, the Linear Filtering Technique (LFT) or the Triple Decomposition Method (TDM) separate out $\tilde{\mathbf{u}}$ from $\mathbf{u}'$. Phase averaging extracts $\tilde{\mathbf{u}}$ using

$$\tilde{\mathbf{u}} = \frac{1}{N}\sum_{n=0}^{N-1}\mathbf{u}(\psi_n) \tag{1}$$

over sufficient ensembles N, where ψ_n is the phase of ensemble n. In practice, the phase averaging approach partly leaks a component of $\tilde{\mathbf{u}}$ into the turbulent component due to the random nature of wind waves. On the other hand, the LFT separates $\tilde{\mathbf{u}}$ based on an assumed linear correlation with the water surface elevation, η, dynamic pressure, or another velocity time series measured at a sufficiently close location. The linear correlation assumption of the LFT gives the magnitude squared coherence at frequency ω [3]

$$\gamma^2(\omega) = \frac{|S_{\eta\mathbf{u}}(\omega)|^2}{S_{\eta\eta}(\omega)S_{\mathbf{uu}}(\omega)} \tag{2}$$

where $S_{\eta\eta}(\omega)$ and $S_{\mathbf{uu}}$ are spectral densities and $S_{\eta\mathbf{u}}$ is cross-spectral density of $\mathbf{u}$ and η. The spectra of $\tilde{\mathbf{u}}$ and $\mathbf{u}'$ are then separated by

$$S_{\mathbf{u}'\mathbf{u}'}(\omega) = [1-\gamma^2(\omega)]S_{\mathbf{uu}}(\omega) \tag{3a}$$

$$S_{\tilde{\mathbf{u}}\tilde{\mathbf{u}}}(\omega) = \gamma^2(\omega)S_{\mathbf{uu}}(\omega) \tag{3b}$$

The linear assumption of the LFT decomposes non-linearly correlated wave-induced velocities into the turbulence. This limitation was overcome using stream function theory in the TDM [36]. The TDM separates the non-linearly correlated velocities, as well as irrotational and rotational velocities.

Shonting [32] measured $\overline{\tilde{u}\tilde{w}} \neq 0$ under wind waves using two cylindrical impeller current meters (2D) under wind speeds of *ca.*9 m/s in ca. 7 m water depth. Surprised by the results, Shonting [33] repeated the experiment, recording water velocities using a 2D ducted meter at 5 Hz. Shonting [33] measured wave Reynolds stresses an order of magnitude larger than conventional wind momentum input parameterisations [12]. In addition, Shonting [33] measured downward $\overline{w}$ in order of *ca.* 5 cm/s, possibly due to Langmuir circulations [38].

In another field experiment conducted at the Consiglio Nazionale delle Ricerche oceanographic tower, Cavaleri and Zecchetto [4] measured 2D velocities and water surface elevation using two electromagnetic current meters and a resistance wave gauge in 16 m water depth. The Cavaleri and Zecchetto [4] measurements were conducted at −4.4 m under $H_s = 1.9$ m and $T_p = 6$ s waves where H_s is the significant wave height and T_p is the peak wave period. Easterly winds of 12-17 m/s were well aligned with the wave propagation direction. Cavaleri and Zecchetto [4] measured η and $\tilde{w}$ almost in quadrature but they measured $\tilde{u}$ lagging *ca.* $\pi/6$ behind η. Such a large phase shift resulted in extraordinarily large wave Reynolds stresses, with $-\rho\overline{\tilde{u}\tilde{w}}$ of order 70 Pa. Cavaleri and Zecchetto [4] found $-\overline{\tilde{u}\tilde{w}}$ directly proportional to the wave height. Interestingly, negligible $\overline{\tilde{u}\tilde{w}}$ was measured in swell conditions with the identical experimental setup.

On the other hand, Battjes and van Heteren [2] could not repeat the results of Cavaleri and Zecchetto [4]. Battjes and van Heteren [2] measured 3D water velocities and water surface elevation on an offshore platform located in the southern North Sea in *ca.* 17 m water depth. Their measurements under wind speeds up to 20 m/s do not support the phase shifts measured by Cavaleri and Zecchetto [4], i.e. they found horizontal and vertical orbital velocities almost in quadrature and therefore $\overline{\tilde{u}\tilde{w}} \sim 0$.

Cheung [5] and Cheung and Street [6] conducted a series of experiments in a wind-wave flume 35 m long,0.9 m wide and 1.9 m high with a water depth of 1 m. The experiments covered both purely wind generated waves (at 1.5, 2.6, 3.2 and 4.7 m/s wind speeds) in addition to monochromatic mechanically generated wind-forced waves (at 1.7, 2.5, 4.1 and 6.2 m/s wind speeds). Water surface elevation and water velocities were recorded at 13 m fetch using capacitance wave gauges and a two component Laser Doppler Velocimeter. Data were recorded at 100 and 200 Hz. Time averaging and phase averaging were used to separate mean and periodic velocities. For pure wind waves, Cheung and Street [6] measured positive $\rho\overline{\tilde{u}\tilde{w}}$ with values up to 80% of their estimated wind momentum input. Thus, the data imply transfer of momentum upward, which was unexpected for growing wind waves. The measured $\overline{\tilde{u}\tilde{w}}$ depth distributions followed an exponential distribution of e^{2kz}, where k is wave number. For wind-forced mechanically generated waves, $\rho\overline{\tilde{u}\tilde{w}}$ was measured to be an order of magnitude larger than the measured ρu_{*w}^2 for wind speeds above 4 m/s where u_{*w} is the water side friction velocity. The momentum flux direction was again upward. The extraordinarily large $\overline{\tilde{u}\tilde{w}}$ measured by Cheung [5], although of opposite sign to that expected, was nominated as a possible energy transfer mechanism from waves into the mean flow by $\overline{\tilde{u}\tilde{w}}\frac{\partial u}{\partial z}$ in Grare et al. [10]. This was to compensate for a significant wave energy loss downwind, in comparison to the air-side measured wind energy input into the waves.

Thais and Magnaudet [37] investigated the structure of the